EC5 and probabilistic based design of a composite T beam

L.M.C. Simões and A.V. Lopes
Dep.Civil Engineering , University of Coimbra – Polo II, 3030 Coimbra - PORTUGAL

Abstract
The design of a T beam based on both EC5 and the probabilistic model code are compared. The cross section consists of a composite section made of lightweight aggregate concrete built on a Glulam LC beam. Steel connectors are used. The lightweight concrete can be characterized as of class LC20/22. The glulam used is of class GL24h and the wood is class C18. Data on moisture content (both before and after casting), E, ρ of several beams were used to evaluate the probabilistic data. The EC5 design involves both the strength of the materials and connections. The probabilistic model considers bending, shear strength, interaction between these modes and the shear of the connection as limit states. A level II procedure is employed to evaluate the reliability indices and the overall probability of failure is found by employing Ditlevsen bounds. Examples are given illustrating the influence of the variability of the loading and material on the probability of failure.

Key words: timber-concrete composite structures, screw type connections, lightweight concrete, probabilistic-based design

1. Introduction
Timber-concrete composite structures deal with the coupling of two materials with different mechanical properties, connected by mechanical fasteners or other connection system. The composite system produces a cross-section with a good balance between strength, stiffness and self weight when compared with similar structural solutions designed from each material component alone.

The use of light-weight aggregates concrete (LWAC) instead of normal-weight concrete in timber-concrete composite structures allows for an important reduction of dead load.
Not many studies have so far specified the use of lightweight concrete in timber-concrete composite structures. The experimental program reported here has been developed at the University of Coimbra and concerns short and long term shear tests on the connection and the structural behaviour of T-beams.

The cross section type used is illustrated in Fig. 1 and the connection system is produced by special screws (SFS VB 48x7.5x100) positioned as in Fig. 2.

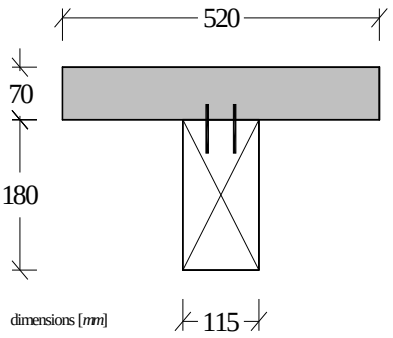

Fig. 1 TCC cross section used in experimental work.

The lightweight concrete fits to density class D1,6 and strength class LC 20/22 according to EN 206-1 [1].

Fig. 2 Position of the screws used.

The aggregate used in this work is Portuguese LECA® and the concrete mix used maximized the concrete strength into a level similar to normal concrete used.

2 Materials

The connection is made by special screws (SFS VB 48x7.5x100)

ϕ (mm)	L (mm)	E (KPa)	t1 (mm)	t2(mm)	fu (MPa)
8	150	2,10E+08	50	100	600

Table 1 Connections

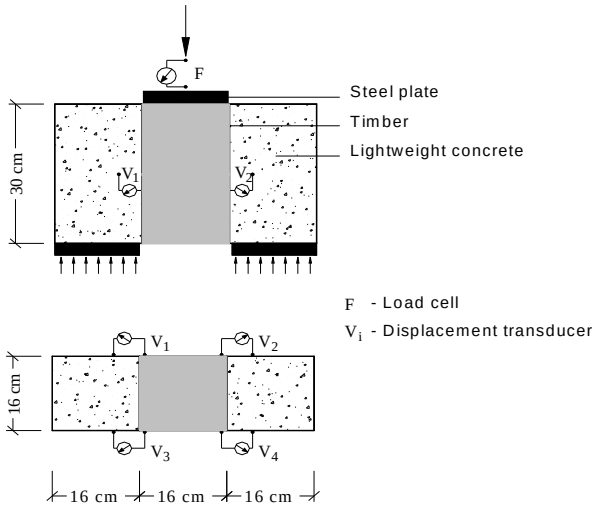

Fig.3 Shear test setup

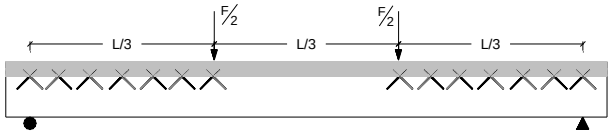

Fig. 4 Static setup for the bending tests.

Timber glued laminated spruce was employed. The beams were subjected to tests, which lead to the parameters reported in Table 2.

The moisture content and density of timber were determined just after tested, from 4 specimens randomly picked from the 20 tested. (a) refers to moisture content after assembling the composite beam and (b) is the moisture content given the lab conditions.

Beam	E (Gpa)	ρ (Kg/m3)	H_20 (a)	H_20 (b)	Class	
V1	9.8	399	11,4	14,45	C18	GL 24h
V3	10.3	395	12	13,25		
V4	11.35	406	10,5	12,4		
V5	14.45	420	11,8	13,65		

Table 2 Glulam

The compression strength and density of the lightweight concrete was derived from 6 cubes tested simultaneously to the shear tests on the connections, which took place between 28 and 35 days after casting the composite specimens. Their results just meet requirements of strength class LC 20/22 (f_{lcm} =29.6MPa) and density class D1.6.

Slab	fm(Mpa)	σ (Mpa)	Ω	ρ (Kg/m3)	Class	
L4	29.1	2.16	0.074	1550	1.6	L 20/22

Table 3 Lightweight concrete (LWAC):

3. Eurocode 5 (EC5) criteria for design

3.1 Internal Stresses

The stresses on the composite section were obtained via Annex B of EC5 (deflections due to bending moments). If one of the materials is the LWAC, the normal stresses can be obtained as,

$$\sigma_i = \frac{\gamma_i E_i a_i M}{(EI)_{ef}} \tag{2a}$$

$$\sigma_i = \frac{0.5 E_i h_i M}{(EI)_{ef}} \tag{2b}$$

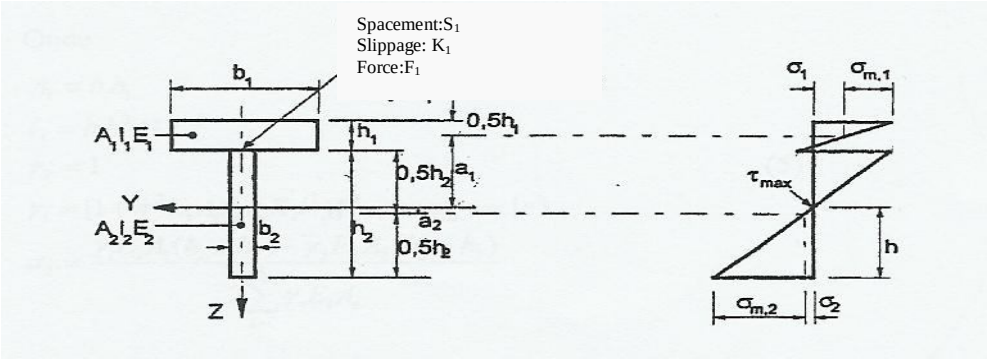

Fig. 5 Annex B (EC5)

There are four limit states involving concrete resistance to compression/tension (upper/lower fibre) and wood resistance to compression/tension (upper/lower fibre).
The shear stress on the wood is defined by eq. (3),

$$\tau_{2,\max i} = \frac{\gamma_3 E_3 A_3 a_{3+0.5E_2 b_2 h^2}}{b_2 (EI)_{ef}} V \tag{3}$$

These stresses are determined by using an effective flexural stiffness, which is also given in Annex B

$$(EI)_{ef} = \sum_{i=1}^{3} (E_i I_i + \gamma_i E_i A_i a_i^2) \tag{4}$$

where,

$$
\begin{aligned}
A_i &= b_i h_i \\
I_i &= b_i h_i^3 / 12 \\
\gamma_i &= \left[1 + \pi^2 E_i A_i s_i / (K_i l^2\right]^{-1}, \; para\_i = 1e3 \\
a_2 &= \frac{\gamma_i E_i A_i (h_1 + h_2) - \gamma_3 E_3 A_3 (h_2 + h_3)}{2 \sum_{i=l}^{3} \gamma_i E_i A_i}
\end{aligned}
\tag{5}
$$

3.2 Connection forces

The connections are verified to satisfy pure shear by considering several possible failure modes. These depend on the penetration lengthy of the connector in the different materials (t_1, t_2) the strength to localized crushing in t_i ($f_{h,1,d}$, $f_{h,2,d}$), the connector diameter (d) and the plastic yielding moment of the connector ($M_{y,d}$)

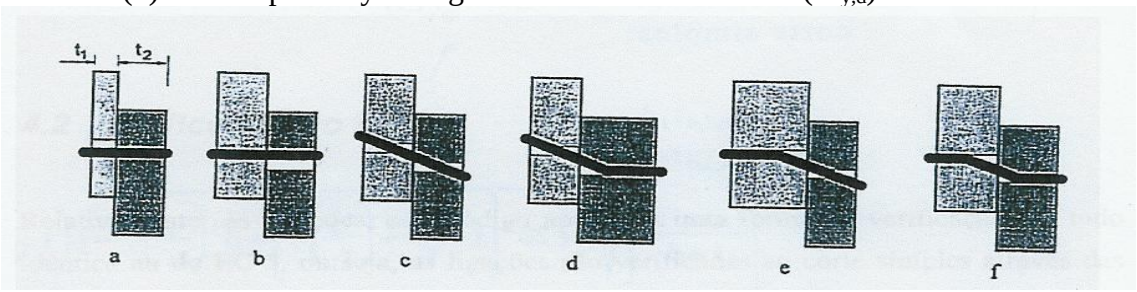

Fig. 6 Failure modes due to shear

The shear force is then the minimum out of the following expressions,

$$
R_k = \min \begin{cases}
f_{h,1} t_1 d \\
f_{h,2} t_2 d \\
\dfrac{f_{h,1} t_1 d}{1+\beta} \left[\sqrt{\beta + 2\beta^2 \left[1 + \dfrac{t_2}{t_1} + \left(\dfrac{t_2}{t_1} \right)^2 \right] + \beta^3 \left(\dfrac{t_2}{t_1} \right)^2} + \beta \left(1 + \dfrac{t_2}{t_1} \right) \right] \\
\dfrac{f_{h,1} t_1 d}{2+\beta} \left[\sqrt{2\beta(1+\beta) + \dfrac{5\beta(2+\beta) M_{y,k}}{f_{h,1} d t_1^2}} - \beta \right] \\
\dfrac{f_{h,1} t_1 d}{1+2\beta} \left[\sqrt{2\beta^2(1+\beta) + \dfrac{5\beta(1+2+\beta) M_{y,k}}{f_{h,1} d t_2^2}} - \beta \right] \\
1.15 k_{cal} \sqrt{\dfrac{2\beta}{1+\beta}} \sqrt{2 M_{y,k} f_{h,1} d}
\end{cases}
\tag{6 i, i=a,…,f}
$$

Given the pre-drilling of the connectors,

$$f_{h,k} = 0.082\,(1\text{-}0.01\,d)\,\rho_k \quad \text{and} \quad \beta = f_{h,2}/f_{h,1} \tag{7}$$

The plastic yielding moment of the connector is given by,

$$M_y = 180\, d^{2.6} f_u / 600 \tag{8}$$

and the forces acting on the connectors are,

$$F_y = \frac{\gamma_i E_i A_i a_i s_i}{(EI)_{ef}} V \qquad where \qquad i = 1e3 \tag{9}$$

3.3 Composite beam design

The static loading is given in Table 4,

P (kN/m)	M_{max} (kNm)	V_{max} (kN)
4.50	16.40	12.15

Table 4 Loading, bending moment and shear

By using Annex B of EC5 one obtains the following stresses for concrete:

Concrete:LC20/22											
b (m)	hi (m)	E (kPa)	A (m^2)	I (m^4)	P (Kg/m^3)	γ	a_1 (m)	σ_1 (MPa)	σm_1 (MPa)	$\sigma_{1+}\sigma m_1$ (MPa)	σ_{1t} (MPa)
0.52	0.07	1.4E+07	0.0364	1.49E-05	1500	0.646	0.051	2.591	2.75	5.34	0.156

Table 5 Concrete stresses

The stresses in the Glulam LC are,

Glulam:GL-24h													
b (m)	hi (m)	E (kPa)	A (m^2)	I (m^4)	ρ (Kg/m^3)	γ	a_2 (m)	σ_2 (MPa)	σm_2 (MPa)	h (m)	$\sigma_{2+}\sigma m_2$ (MPa)	σ_{2c} (MPa)	τ_2 (MPa)
0.115	0.18	1.1E+0.7	0.0207	5.59E-05	400	1	0.074	4.556	5.551	0.164	10.107	0.995	0.613

Table 6 Glulam GL stresses

The resisting stresses in the concrete and Glulam are obtained by using the mechanical characteristics of the materials,

Concrete:LC20/22							
α_c	γ_c	f_{clm} (MPa)	f_{clk} (MPa)	f_{cld} (MPa)	f_{cltm} (MPa)	f_{cltk} (MPa)	f_{cltd} (MPa)
0.8	1.5	28	20	10.67	1.78	1.21	0.807

Table 7 Resisting stresses on the concrete

Glulam:GL-24h						
K_m	K_{mod}	γ_m	f_{myk} (MPa)	f_{myd} (MPa)	f_{tmyk} (MPa)	f_{tmyd} (MPa)
0.7	0.8	1.3	24	14.77	16.5	10.2

Table 8 Resisting stresses on the Glulam LC

By using the results from Tables 5-8,

Criteria	S_d(MPa)	R_d(MPa)	S_d/R_d
σ 1(-)	5.34	10.67	0.50
σ 1(+)	0.16	0.81	0.19
σ 2(-)	1.00	14.77	0.07
σ 2(+)	10.11	10.2	0.99
τ2	0.61	2.7	0.23

Table 9 Limit states for the stress

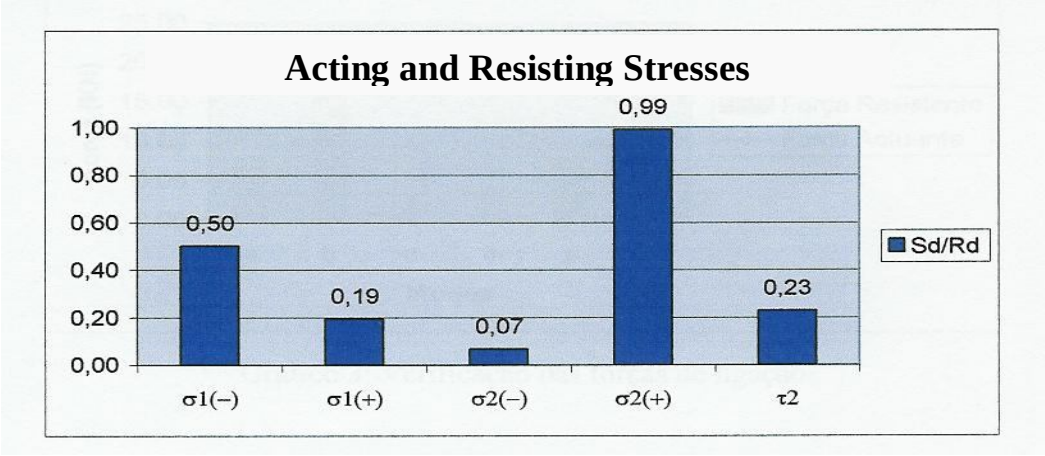

Fig. 7 Acting/resisting stresses

The acting forces in the connection were obtained by using eq. (9) and were compared with those obtained by employing a finite element modelling

Nº connectors	F_1	F_2	F_{fe}
2	6,99	6,99	6,76
1	3,49	3,49	3,38

Table 10 Acting force on the connectors

	f_{h1k} (MPa)	f_{h2k} (MPa)	β	γ_m	M_{yk} (Nmm)	M_{yd} (kNm)	K_{cal}
ϕ >8mm	20.00	30.18	1.51	1.1	40115.0	36468.2	1.3

Table 11 Parameters used to find the resisting force

	MODES(kN)					
	a	b	c	d	e	F
ϕ >8mm	8.00	24.14	9.47	3.85	7.89	5.87

Table 12 Resisting Force

Fig 8 compares the acting and resisting force in the connection.

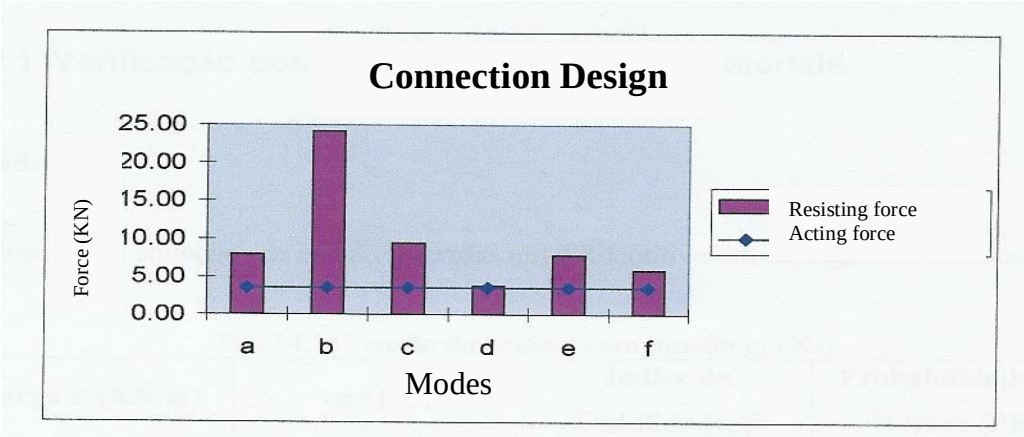

Fig.8 Connection forces checking

4. Probabilistic Based Design

According to the probabilistic model code (PMC) the wood properties more intensely studied experimentally given its inherent variability are the flexural stress (f_m), Young modulus (E_m) and density (ρ_o). Concerning the variation of these parameters: a) f_m may occur at a finite number of (weak) sections; b) although E_m is usually considered discrete at elementary level, variations along the elements can be considered, the length in which there exists variability being given by eq.10; c) ρ_o is modelled as a normal random variable and can be correlated with other material properties.

$$l_{ij} = \frac{(t_{ij} - t_{ij-1})}{2} + \frac{(t_{ij+1} - t_{ij})}{2} \qquad (10)$$

Glulam LC data is not yet provided in the PMC.

This model code presents a similar way of designing connections as in EC5, given they are verified to simple shear by using Johansen equations (6i). Here, according to Blass,

$$M_y = 0.3 f_u d^{2.6} \qquad (11)$$

Consistent with the first order second moment approximation (FOSM), the probability of failure can be written in terms of the linear safety margin of a limit state function g(x) of normal random variables x as:

$$P_F = P\{g(x) \le 0\} \quad (12)$$

which reduces to the evaluation of the standard normal distribution function,

$$P_F = \Phi(-\beta) \quad (13)$$

where β is the reliability index. The reliability index has the geometrical interpretation as the smallest distance from the boundary between the safe domain and the failure domain. The evaluation of the probability of failure reduces to simple evaluations in terms of mean values and coefficients of variation of the basic random variables. In the following example uncorrelated normal variables are used.

Material		μ	Ω	σ
Concrete (mat.1)	f_1(MPa)	29.1	0.15	4.37
	f_{t1}(MPa)	1.78	0.2	0.36
	$f_{h,1}$(MPa)	28	0.15	3.30
Wood (mat.2)	f_2(MPa)	31.2	0.14	4.37
	f_{t2}(MPa)	21.5	0.14	3.01
	τ_2(MPa)	3.5	0.14	0.49
	ρ(Kg/m^3)	405	0.05	20.25

Table 13 Parameters used in the reliability analysis

4.1 Limit state functions

The limit state functions associated with stresses can be written as,

$$g_i = X_i - K_i P \ge 0 \quad (13)$$

where X_i represent the yield stress of material i and K_i P is the stress in the same material and fibre due to the loading P. The limit states due to connection forces are developed in a similar way as given in (6i).

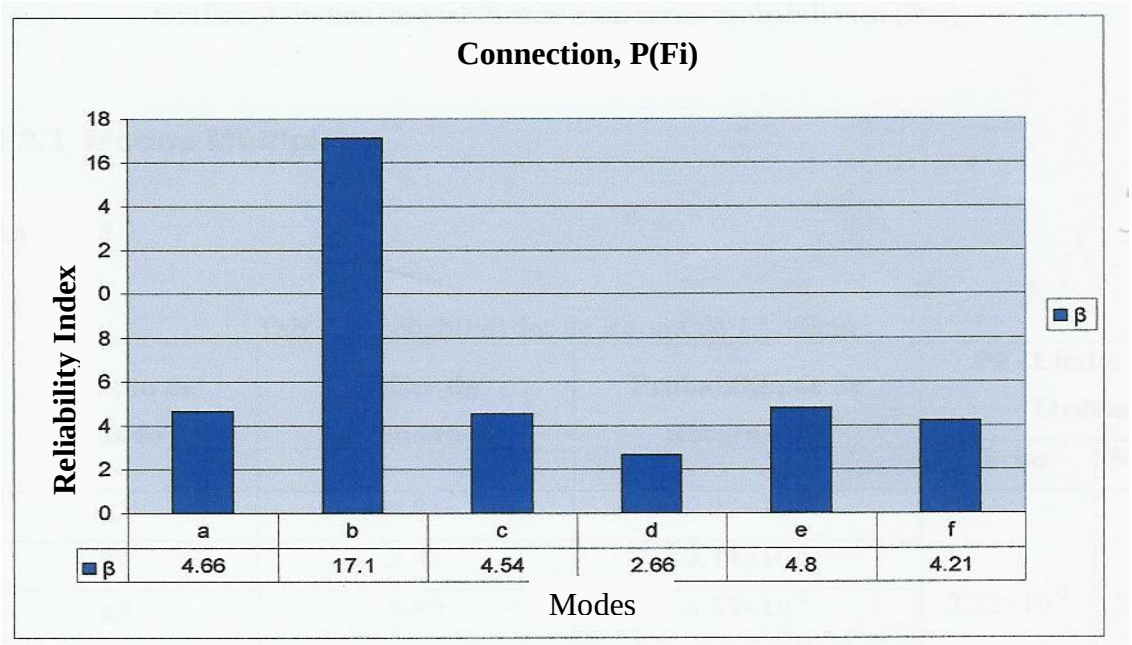

Fig.9

The reliability indices obtained for the several failure scenarios associated with the shear force of the connections for deterministic P are represented in Fig.9 and the following graphic displays the effect of different cov of the loading on the reliability indices.

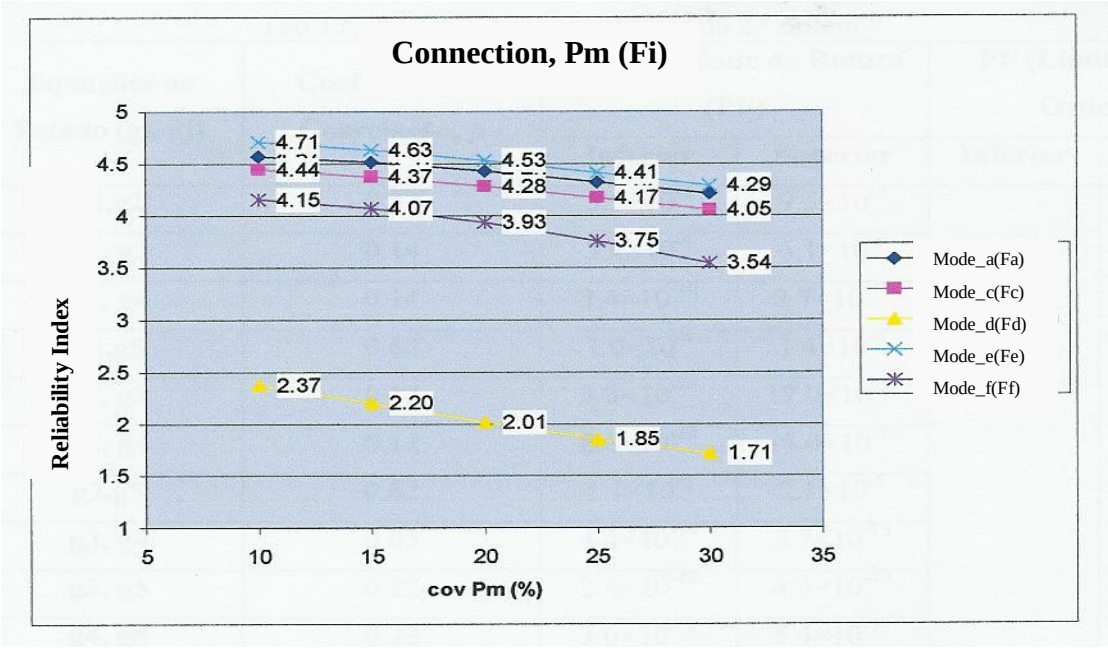

Fig.10

The most likely failure due to shear force of the connection (mode d) is given by,

$$g_1(X_i) = \frac{f_{h,1} t_1 d}{2+\beta}\left[\sqrt{2\beta(1+\beta) + \frac{5\beta(2+\beta)M_y}{f_{h,1} d t_1^2}} - \beta\right] - 0.775P \qquad (15a)$$

Fig. 11 shows the reliability indices obtained for the several failure scenarios associated with the stresses due to bending when P is fixed.

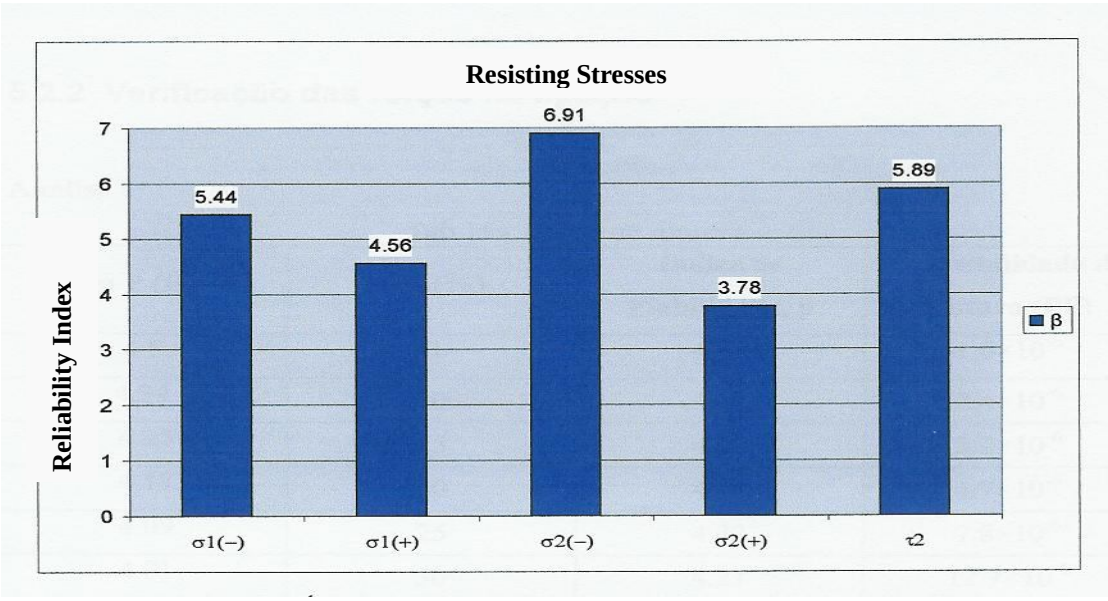

Fig.11

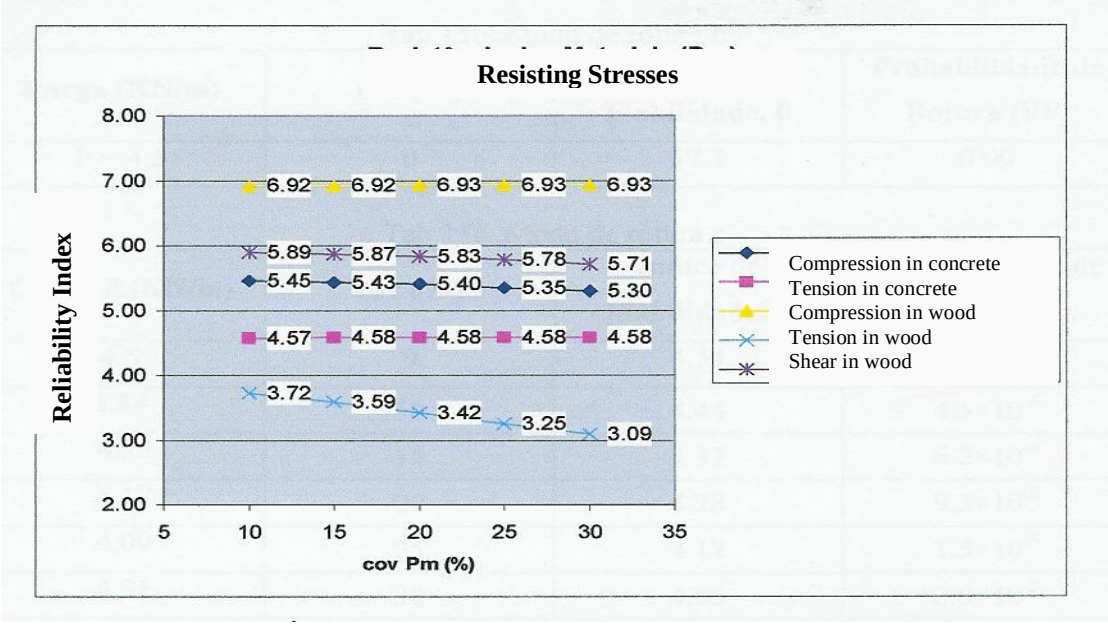

Fig.12 Effect of different cov of the loading on the reliability indices

By using the results obtained so far, the most important modes due to bending are:
Tension stresses in the wood,

$$g_2(X_i) = M_2 - \frac{PL^2}{8} \tag{15b}$$

Compression stresses in the concrete,

$$g_3(X_i) = M_1 - \frac{PL^2}{8} \tag{15c}$$

Shear stress on the wood,

$$g_4(X_i) = V_2 - \frac{PL}{2} \tag{15d}$$

The interaction flexure-shear on the wood should also be considered as a limit state,

$$g_5(X_i) = 1 - \left(\frac{L^2 P}{8M_2} + \frac{M_2 P}{2V_2^2} \right) \tag{15e}$$

4.2 Structural Reliability

A first estimate of p_F can be found through well-known first-order bounds proposed by Cornell. The lower bound, which represents the probability of occurrence of the most critical mode (dominant mode) is obtained by assuming the mode failure events g_k to be perfectly dependent, and the upper bound is derived by assuming independence between mode failure events. Hence, approximation by Cornell's first-order upper bound is very conservative because it neglects the high correlation between failure modes. Improved bounds can be obtained by taking into account the probabilities of joint failure events. The resulting closed-form solutions for the lower and upper bounds are as follows:

$$p_F \geq (g_1) + \sum_{i=2}^{m} Max\left\{ \left[P(g_i) - \sum_{j=1}^{i-1} P(g_i \cap g_j) \right]; 0 \right\} \tag{16a}$$

$$p_F \leq \sum_{i=1}^{m} P(g_i) - \sum_{i=2}^{m} Max_{j<i} P(g_i \cap g_j) \tag{16b}$$

The above bounds can be further approximated using Ditlevsen's method of conditional bounding to find the probabilities of the joint events. This is accomplished by using a

Gaussian distribution space in which it is always possible to determine three numbers β_1, β_2 and the correlation coefficient ρ_{ij} for each pair of collapse modes g_i and g_j.

If the parameters of Table 13 and a cov of 0.2 for the loading are used, the overall probability of failure of the composite beam is given in Table 14.

Limit state equations (gi, gj)	**Correlation coefficients, ρ**	**Joint Probability of Failure (P_F)**		**P_F (2nd Order bounds)**	
		Lower	**Upper**	**Lower**	**Upper**
g1,g2	0.33	$5.5\text{x}10^{-5}$	$9.5\text{x}10^{-5}$	$2.24\text{x}10^{-2}$	$2.25\text{x}10^{-2}$
g1,g3	0.14	$3.4\text{x}10^{-9}$	$6.1\text{x}10^{-9}$		
g1,g4	0.14	$2.4\text{x}10^{-10}$	$2.7\text{x}10^{-10}$		
g1,g5	0.62	$1.0\text{x}10^{-4}$	$1.4\text{x}10^{-4}$		
g2,g3	0.12	$9.3\text{x}10^{-11}$	$17.0\text{x}10^{-11}$		
g2,g4	0.12	$8.6\text{x}10^{-12}$	$16.0\text{x}10^{-12}$		
g2,g5	0.62	$1.1\text{x}10^{-5}$	$2.1\text{x}10^{-5}$		
g3,g4	0.05	$4.4\text{x}10^{-16}$	$8.7\text{x}10^{-16}$		
g3,g5	0.22	$2.4\text{x}10^{-10}$	$4.3\text{x}10^{-10}$		
g4,g5	0.23	$3.0\text{x}10^{-11}$	$5.4\text{x}10^{-11}$		

Table 14

This example shows that the limit state associated with the connection forces is dominant.

Acknowledgements
The authors would like to acknowledge the important contribution of L. Jorge, H. Costa and C. Diogo Gomes in this work.

References

[1] EN 206-1, Concrete Part 1: Specification, performance, production and conformity, CEN. 2000.

[2] EN 384 – Structural timber, Determination of characteristic values of mechanical properties and density, CEN. 1995.

[3] EN 408 – Timber structures, Structural timber and glued laminated timber – Determination of some physical and mechanical properties, CEN. 1995.

[4] prEN 1992-1 – Eurocode 2: Design of concrete structures - Part 1.1: General rules and rules for buildings, CEN. April 2003.

[5] prEN 1995-1-1 – Eurocode 5: Design of timber structures - Part 1.1: General rules and rules for buildings, CEN. October. 2003.

[6] L. Jorge, S. Lopes, S. and H. Cruz, Experimental Research in Timber-LWAC composite structure, COST E29 Symposium, Florence 27-29 October 2004.

[7] J. Kohler and M.H. Faber, Probabilistic Model Code for Design of Timber Structures, Draft, ETHZ, April 2004.

[8] H. Blass, H. et al, Trag und verformungsverhalten von holz-beton-verbundkonstruktionen, TH Karlsruhe, Germany, 1995.

[9] A.Ang and W. Tang, Probability Concepts in Engineering Planning and Design, J. Wiley & sons, 1984.